# Silicon Low Power, Low Voltage MEMS Switches for Space Communication Systems

**R.W. Moseley[1], E.M. Yeatman[1,2], A.S. Holmes[1,2], R.R.A. Syms[1,2], A.P. Finlay[1], P. Boniface[3]**

[1]*Microsaic Systems Ltd, GMS House, Boundary Road, Woking, Surrey, GU21 5BX, UK*
[2]*Imperial College London, EEE Department, London SW7 2BT, UK*
*Email:rmoseley@microsaic.com*
[3]*EADS-Astrium Ltd, Anchorage Road, Portsmouth, PO3 5PU, UK*

## ABSTRACT

This paper describes a MEMS RF switch designed and developed specifically for space communication systems, with a novel geometry and operating mode that overcome the drawbacks of previous devices. To avoid the need for high voltage control, the switch uses electro-thermal rather than electrostatic operation; although this requires higher power consumption during switching, a latching configuration was used such that the hold power is zero in either switch state. This requires that the actuation is lateral (with respect to the chip surface) rather than vertical as in most MEMS switches. Lateral actuation allowed a large open-state separation to be achieved, leading to high-isolation performance. The latching operation also inherently provides high mechanical stability.

While most reported MEMS switches have been 2-port series or shunt switches, the system requirement addressed here was for a 3-port, single-pole double-throw (SPDT) switch (i.e. one input, two selectable outputs). To keep the device compact, this necessitated the use of strongly confining transmission lines, so thin-film microstrip (TFMS), rather than coplanar waveguides (CPWG), was used. By integrating low-loss TFMS with our novel MEMS switch geometry, the SPDT switch operation was achieved with good initial performance, including operating voltage 3 V, isolation 50 dB and insertion loss 1.8 dB at 5 GHz, and operating range 1-20 GHz. Packaging of the devices was carried out using a CPWG alumina cavity package.

## 1. INTRODUCTION

Requirements for switching in the radio frequency (RF) and microwave regime, in space systems, are becoming increasingly demanding as the systems grow in complexity. Key among these requirements are low power operation, low signal loss, high isolation, and broadband operation. MEMS technology offers significant performance advantages over conventional solid state switches for all these requirements [1,2]. Although switching speeds are modest (typically milliseconds), this is adequate for many reconfiguration applications, e.g. in phased array radar or in multi-channel communication systems. However, MEMS switches reported to date, targeted primarily at terrestrial applications, also have characteristics which make them unsuitable for space deployment; in particular, the need for high voltage controls, and excessive vibration and shock sensitivity.

To overcome these disadvantages we have developed a novel MEMS switch utilising lateral rather than vertical actuation, with mechanical latching to maintain the state without actuator power [3]. Direct contact rather than capacitative connection results in broadband operation down to DC, suitable for digital (baseband) as well as analogue signals. The RF transmission line used were thin-film micro-strip (TFMS), with dimensions and composition that give a characteristic impedance of 50 Ω, necessary for low-loss connection to standard equipment. Other transmission lines (such as coplanar waveguide) were investigated, but found to offer less favourable electrical performance, e.g. co-planar waveguides require excessively large gaps between the signal lines and relay to give sufficient RF isolation.

## 2. SWITCH LAYOUT AND OPERATION

The switch layout and principles of operation can be seen in Figure 1. A relay “plunger” is moved laterally to bridge a gap between two parts of the signal line. This plunger is connected, via a double flexible cantilever support, to a thermal actuator. This actuator operates by passing a current between the contact pads at its base; this current passes consecutively through the two “hot arms” extending from the contact pads which are joined at their upper, moving end. The relatively high electrical resistance of these hot arms causes them to heat and expand when the current is applied; an additional anchor point provides a pivot point, causing the actuator end to move laterally. This then pushes against the upper, free end of a lower double flexure (portal frame), so that it displaces. The upper flexure to which the plunger is attached is connected to this lower flexure in a rigid well; this is done to reduce the overall device length. The upper

flexure is required so that the plunger lakes contact with the signal line gap before the latch parts engage; once the actuator pushes the latch fully into place, the deflection of this upper flexure ensures that a suitable contact force is maintained. An additional thermal actuator is provided to release the latch for the switch to be opened.

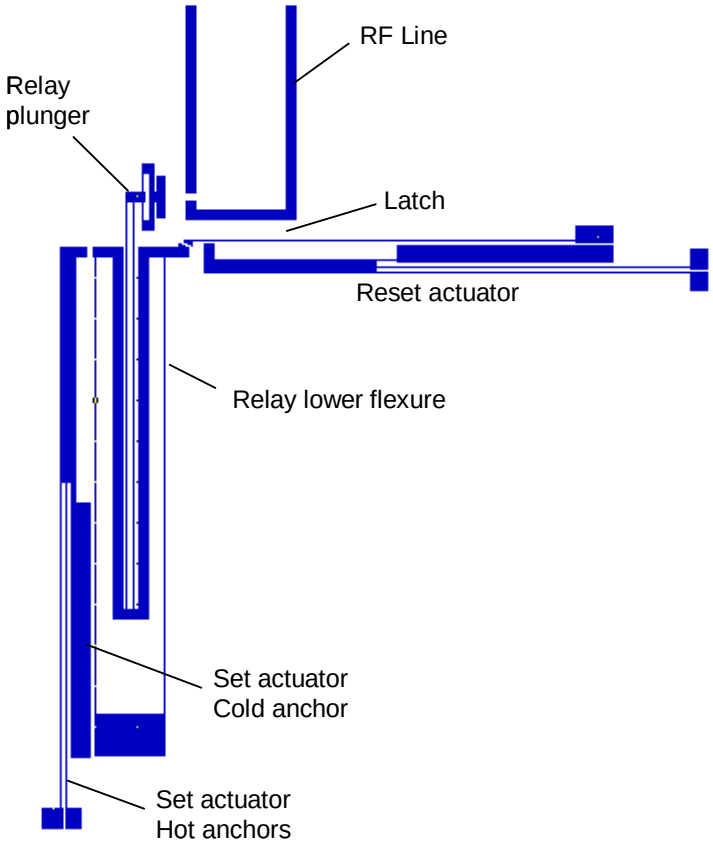


Fig. 1. Schematic of single series switch, showing principle of operation and main structural components.

The operation of the switch can be described with reference to Fig. 2. The switch is initially OFF (top left). In (top right), the set actuator pushes the plunger across the gap in the signal line and starts to engage the latch. Once engaged, the actuator can be released and the switch is held in the ON position without actuator power (bottom right). The switch can then be released by the reset actuator triggering the latch (bottom left) after which the device is back in the OFF state.

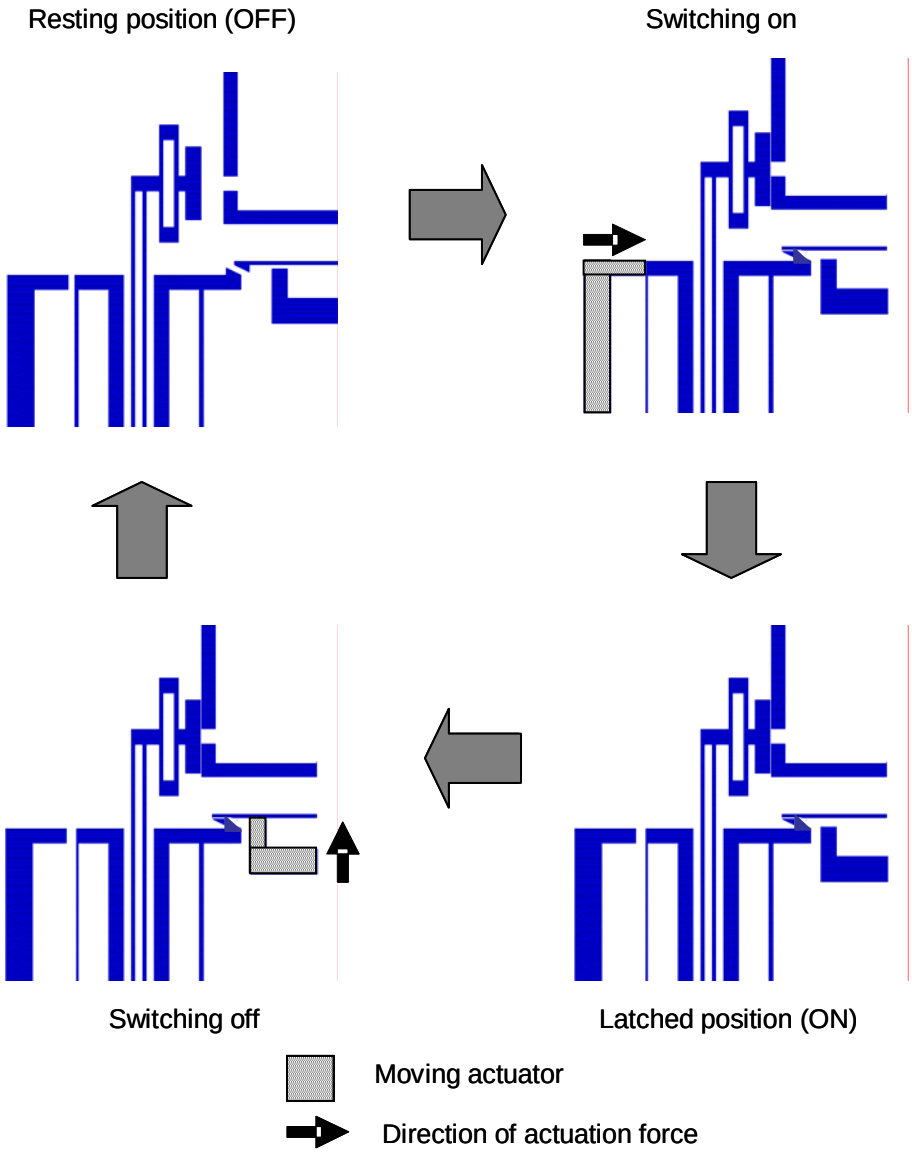


Fig. 2. Schematic showing switching operation.

Further detail of the actuated parts as fabricated can be seen in Figure 3. In this case the full SPDT layout is shown; this consists of a Y-junction in the signal line with gaps in each of the two tributary paths, with a full set of mechanics (set actuator, release actuator, latch) for each path. The length of the signal lines from the Y-junction to the gaps must be minimized, as for each state one of these acts as a stub load on the connected path, and if its length is significant compared to the operating wavelength, an impedance mismatch will be cause, and this will lead to return losses. This problem can also be reduced by using a tuned stub length [4], but this is only suitable for narrow-band operation.

The gaps in the lines must be long enough to ensure high isolation across the open gap. However, since the plunger contact will affect a section of impedance matched line when closed, because of the inevitable difference in geometry, the gap should also be electrically short to avoid reflections. To achieve the short gaps, and allow the stub lengths also to be short, TFMS was chosen for the transmission lines rather than the more commonly used CPWG. TFMS lines are more difficult to fabricate, as they require 3 layers (ground, dielectric and signal), but they have much stronger field confinement than CPWG. They can also be fabricated on lossy substrates such as silicon, although in this case glass was used.

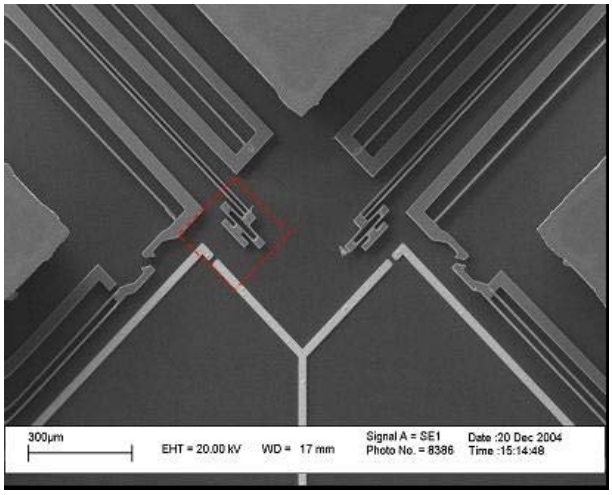


Fig. 3. Scanning electron micrograph of contact area for SPDT switch as fabricated.

## 3. FABRICATION AND ASSEMBLY

The devices were fabricated using a two-wafer approach. The mechanical parts were fabricated in single crystal silicon, using bonded Si-on-insulator (BSOI) wafers. This provides highly reproducible mechanical performance, without the yield, creep and fatigue problems common in metal structures. The poor RF conductance of Si also helps decouple the RF signal from the DC control connections. The TFMS lines, meanwhile, were deposited on glass wafers. While this was not needed for conductivity reasons, as indicated above, the transparency aided in assembling and bonding the two parts after fabrication.

Figure 4 shows the process flow for each of the wafer types, and the final assembly step. The process steps are self-explanatory, and all use standard semiconductor processing equipment and procedures.

The assembly of the RF and mechanical parts of the switch uses an alignment and bonding rig which incorporates the following features:

- Vacuum stage with inspection window for die alignment and heaters for curing;
- 2-stage micropositioner attached to microscope to allow precise alignment of BSOI with TFMS;
- Precision levelling of the BSOI and TFMS using a laser alignment method.

A robust assembly procedure was developed, having the following steps:

1. Level BSOI and TFMS parts;
2. Rough alignment of BSOI and TFMS;
3. Bring TFMS down to near contact with BSOI;
4. Align the alignments marks on the BSOI and TFMS;
5. Bring BSOI down onto TFMS into hard contact, using a calibrated spring-loaded vertical stage and apply a measured constant force;
6. Cure epoxy by heating vacuum stage;
7. Unload switch from vacuum stage.

Figure 5 shows an example of an assembled die.

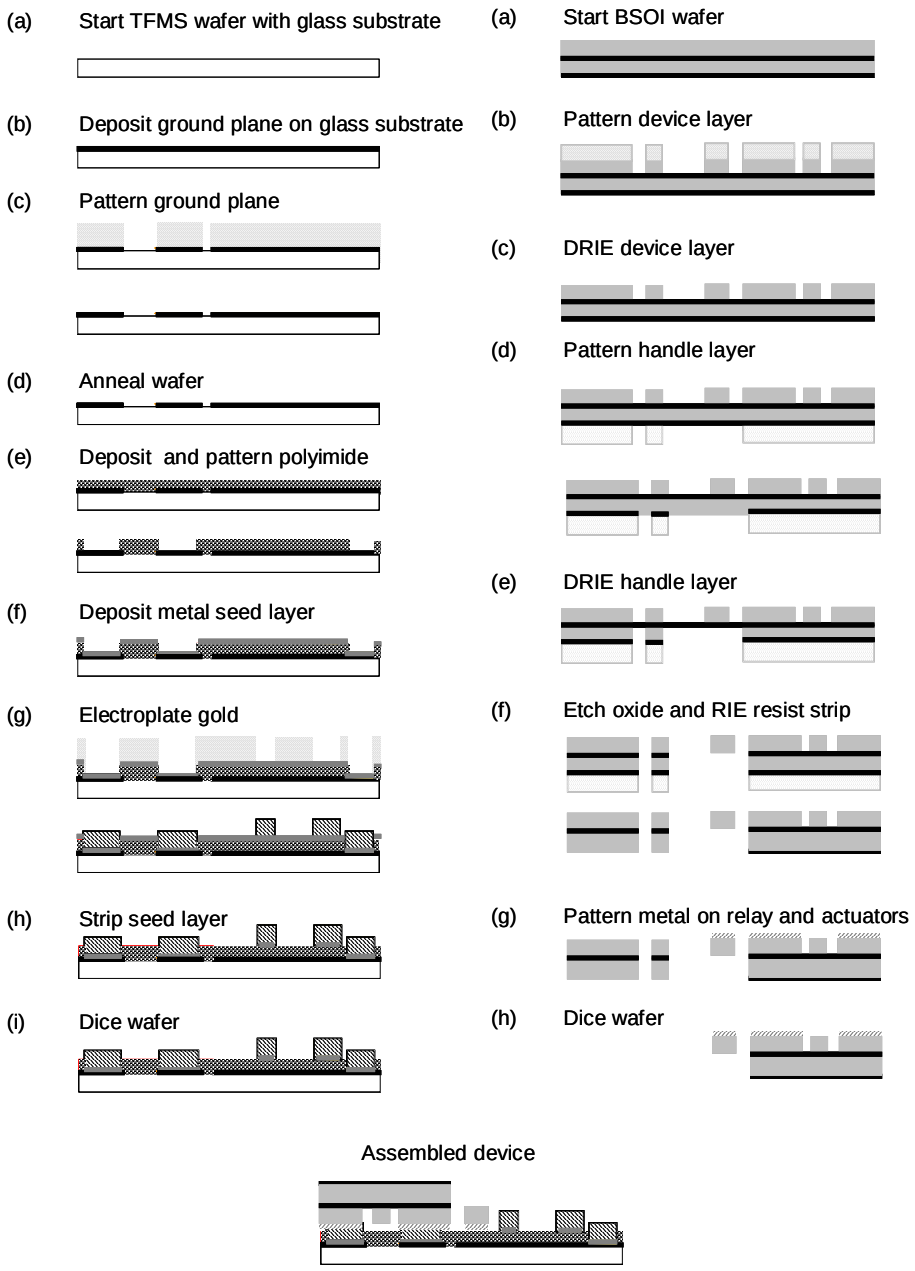


Fig. 4. Process steps for switch fabrication, with steps for the RF lines on the left and those for the mechanical parts on the right.

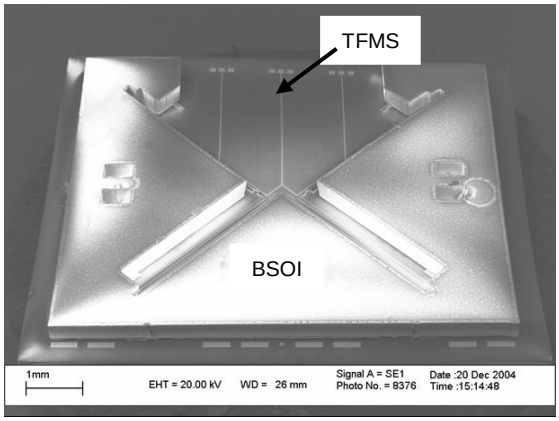


Fig. 5. Scanning electron micrograph of assembled device, with the BSOI mechanical die on top and the glass die with the TFMS lines below. The DC contact points are visible on the lower edge of the TFMS die.

Finally, the devices are packaged, using a CPWG alumina cavity package. This is shown in Figure 6. Bond pads for DC (control) and RF contacts are incorporated on opposite sides of the package.

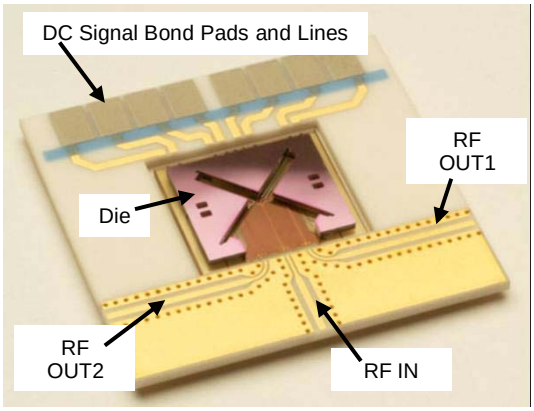


Fig. 6. Photograph of the packaged switch

## 4. TESTING AND EVALUATION

RF losses and isolation of a fabricated (unpackaged) switch were recorded using the open and closed output ports. Measurements were taken using a summit probe station and HP8753D VNA. A TRL calibration was used to de-embed the losses and isolation. Figure 7 shows the losses obtained for a measurement range 0 – 6 Ghz. Although the insertion losses are reasonable, they are well below what can be achieved with MEMS switches. The reason can be seen with reference to Fig. 5. In order to bring the RF lines to the upper edge of the die, while still leaving space for the mechanical actuators, a high TFMS path length of c. 8 mm was needed. Good performance was achieved for the TFMS propagation losses, as is shown in Fig. 8; after modification of the signal line deposition process to eliminate under-plating, the losses were near the modelled values. However, TFMS is inherently a relatively high loss type of line, and 8 mm of propagation accounts for over 1 dB of loss at 5 Ghz. Therefore, in future designs the line length to the bond pads will be substantially reduced. Additional loss is mainly due to contact resistance, which will also be reduced by improved metallization of the plunger connecting surface.

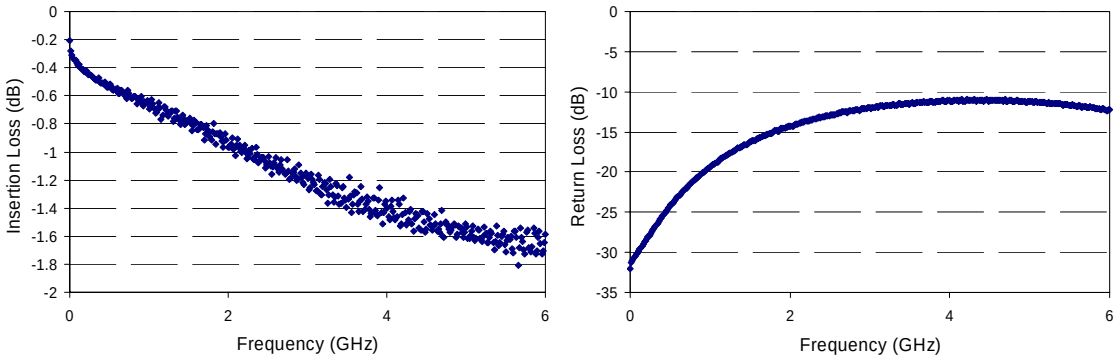


Fig. 7. Measured SPDT switch losses.

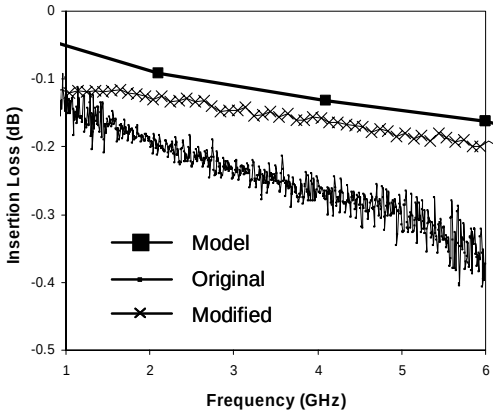


Fig. 8. Measured and modeled TFMS propagation losses.

Isolation values were excellent, as can be seen in Figure 9. This shows the benefits of the TFMS approach, which should also be seen in weak cross-talk between adjacent signal paths.

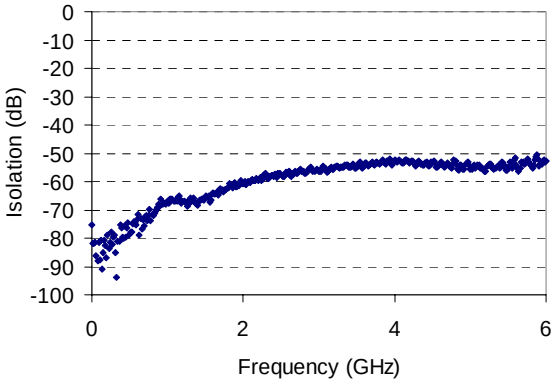


Fig. 9. Measured SPDT switch isolation.

Switching electrical characteristics were also investigated. Both set and trip actuators were found to work effectively with a 3V drive. Figure 10 shows the switch signals; currents of 60 mA were adequate to achieve latching and de-latching, so the actuation instantaneous power is 160 mW. With currents active for 0.5 sec as shown, this indicates a switching energy of 80 mJ; however, switching could be obtained with substantially shorter pulses. This parameter has not yet been systematically characterized.

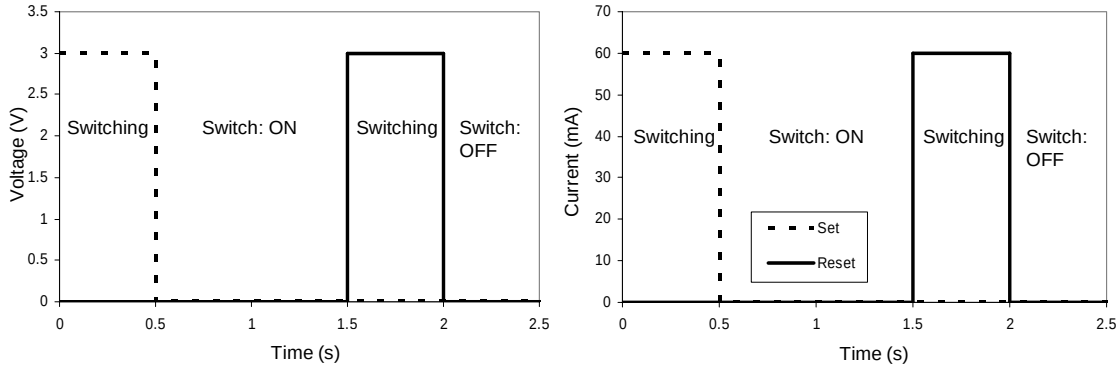


Fig. 10. Electrical DC switching characteristics of the switch showing the currents and voltages required by the set and reset actuators. Less than 100 mJ and a peak power of 100mW are required to switch.

In conclusion, by integrating low-loss TFMS lines with our novel MEMS switch geometry, an SPDT switch has been demonstrated with good initial performance, including operating voltage 3 V, isolation 50 dB and insertion loss 1.8 dB at 5 GHz. Latching for mechanical robustness, and low voltage operation, suggest this device is well suited to space applications.

**REFERENCES**

[1] G.M. Rebeiz, J.B. Muldavin, "RF MEMS switches and switch circuits", IEEE Microwave Magazine vol. 2, pp. 59-71, 2001.

[2] S. Lucyszyn, "Review of radio frequency microelectro-mechanical systems (RF MEMS) technology", IEE Proc. – Science, Measurement and Technology, vol. 151, pp. 93-103, 2004.

[3] M. Geear, E.M.Yeatman, A.S.Holmes, R.R.A.Syms, A.P Finlay., "Microengineered electrically resettable circuit breaker", IEEE/ASME J. MEMS vol. 13, pp. 887- 894, 2004.

[4] M.C. Scardelletti, G.E. Ponchak, N.C. Varaljay, "MEMS, Ka-band single-pole double-throw (SPDT) switch for switched line phase shifters", IEEE Antennas & Prop. Soc. Int. Symp. 2002, Vol. 2, pp. 2-5.